Acta Crystallographica Section C
Crystal Structure Communications
ISSN 0108-2701

$PbZn_{1/3}Nb_{2/3}O_3$ at 4.2 and 295 K

Erich H. Kisi,[a]* Jennifer S. Forrester[a] and Kevin S. Knight[b]

[a]School of Engineering, University of Newcastle, New South Wales 2308, Australia, and [b]ISIS Facility, Rutherford Appleton Laboratory, Chilton, Didcot, Oxfordshire OX11 0QX, England
Correspondence e-mail: erich.kisi@newcastle.edu.au

Received 10 February 2006
Accepted 3 April 2006
Online 24 May 2006

The structure of the relaxor ferroelectric lead zinc niobium trioxide, $Pb(Zn_{1/3}Nb_{2/3})O_3$, known as PZN, was determined at 4.2 and 295 K from very high resolution neutron powder diffraction data. The material is known for its extraordinary piezoelectric properties which are closely linked to the structure. Pseudo-cubic lattice parameters have led to considerable controversy over the symmetry of the structure, which was found to be rhombohedral in the space group *R*3*m* at both temperatures. Atomic coordinates have been determined for the first time. They show that, whereas the deviation of the rhombohedral angle from 90° approaches zero at 295 K, the atomic coordinates do not approach typical cubic positions and hence the polarization remains high.

Comment

Recently, the crystal structures of the perovskite relaxor ferroelectric $Pb(Zn_{1/3}Nb_{2/3})O_3$ (lead zinc niobate or PZN) and its alloys with $PbTiO_3$ (PZN-*x*PT) have been widely debated in relation to the exceptional piezoelectric properties of these materials (*e.g.* Park & Shrout, 1997). A curious aspect of the crystal structure–property relationship in these materials is that the maximum piezoelectric response is along [001], whereas the spontaneous polarization is along [111] of the nominally rhombohedral crystals. Single-domain single crystals are not available and so previous work has relied on synchrotron X-ray (Noheda *et al.*, 2001; Noheda, Cox & Shirane, 2002; Cox *et al.*, 2001) and neutron diffraction (Ohwada *et al.*, 2001) reciprocal-space scans around a limited number of reflections from polydomain single crystals, and on X-ray powder diffraction (Ohwada *et al.*, 2001; Noheda, Zhong *et al.*, 2002; La-Orauttapong *et al.*, 2002). All of the previous experimental studies have dealt only with the lattice symmetry, due to a focus of the work on the polarization rotation hypothesis for the large piezoelectric response (Fu & Cohen, 2000). The materials are pseudo-cubic, making the determination of the true symmetry extremely difficult, even with three-axis diffractometers (Noheda, Zhong *et al.*, 2002). Park & Shrout (1997) first suggested that an electric field-induced phase transition occurred during piezoelectric cycling of PZN-8%PT and that this facilitates the large piezoelectric response. This was rapidly supported by X-ray diffraction studies (Paik *et al.*, 1999; Durbin *et al.*, 1999). The observed symmetry was pseudo-tetragonal. However, Durbin *et al.* (1999) noted that the true symmetry was more likely to be monoclinic. Noheda *et al.* (2001) also concluded that a field-induced transition was responsible and proposed that the monoclinic space group is *Pm*. The same or a very similar mechanism has been proposed for all PZN-*x*PT crystals in the range $0 < x < 9\%$.

The counterpoint has come from Kisi *et al.* (2003) who argued, on group theoretical and physical property grounds, that the large response is more likely to be founded on the very soft elastic constants of the materials than on the lattice symmetry. The observed monoclinic symmetry under an electric field directed along [001] is exactly as expected for the conventional piezoelectric distortion of a rhombohedral crystal. However, this does not constitute a phase transition, nor does it explain the large piezoelectric response. An understanding of the connection between the crystal structure and the piezoelectric properties can only be derived from measured ion coordinates. These can then be used to compute the electric polarization by methods such as that given by Darlington *et al.* (1994).

This paper reports the full crystal structure of the end member, PZN, for the first time. The use of very high resolution neutron diffraction ensures both that the O-ion positions are reliably determined in the presence of far heavier elements such as Pb, and that the problem of pseudo-symmetry is minimized. Data at both 4.2 and 295 K were used to enhance the discrimination between different structural models. Visual inspection of the 111, 200 and 222 reflections in the high-resolution neutron diffraction patterns supported the conventional rhombohedral symmetry. The 111 and 222 reflections are split approximately in the ratio 3:1 and 200 remains unsplit. This aspect has been discussed by Kisi *et al.* (2005) in relation to reports of a cubic '*X*-phase' in this system. Rietveld refinements were initially conducted using the 4.2 K data, due to the larger rhombohedral distortion at this temperature. Refinements in the space group *R*3*m*, illustrated in Fig. 1(*a*), gave reasonable agreement. The major misfit is due to slightly anisotropic reflection widths, in which 200 is broader than 111 by $\simeq 0.2$ times the full width at half-maximum. Geometrically, it is possible for a monoclinic distortion both to split the 111 reflection ($\beta > 90°$) and to broaden 200 ($a \neq b \neq c$) if *a*, *b* and *c* are sufficiently similar. Given that monoclinic phases have been reported in this material, refinements were attempted in all of the monoclinic space groups recently proposed [*Cm*, *Cc* (*Ic*) and *Pm*], with unsatisfactory results. No improvement in the agreement was observed even when a considerable number of extra parameters were added to the refinement. The best fit, shown in Fig. 1(*b*), used the monoclinic structure in *Cm* (Frantti *et al.*, 2003). Octahedral rotation in combination with ferroelectric cation displacements was ruled out by the absence of *R*-point (*e.g. R*3*c*) or *M*-point (*e.g. Cc*) superlattice reflections. This was

  DOI: 10.1107/S0108270106011991

confirmed by Rietveld refinement, which converged to unrotated octahedral positions regardless of the initial conditions. A two-phase mixture of rhombohedral (*R*3*m*) and tetragonal (*P*4*mm*) structures was also tested for completeness. The final refinements were undertaken in *R*3*m* using the anisotropic broadening model of Stephens (1999), as implemented in *GSAS* (Larson & Von Dreele, 1986), to model the effect of interdomain strains due to the microscopic ferroelectric domain structure within the crystallites. Only one additional parameter, S400, was required. The final fit is illustrated in Fig. 1(*c*). A projection of the structure at 4.2 K perpendicular to the polar axis, [111], is illustrated in Fig. 2(*a*) and an equivalent view of the undistorted cubic structure is shown in Fig. 2(*b*). The Pb atoms are aligned, illustrating the large relative displacement of the Zn/Nb and O ions.

Structure refinements using the 295 K data were undertaken using the 4.2 K structure as a starting point. The refined structure at 295 K is the same as that at 4.2 K, with slightly reduced rhombohedral distortion and cation displacements. The departure of the rhombohedral angle from 90° diminishes with increasing temperature as the transition to cubic at approximately 400 K is approached. However, the atom coordinates remain relatively unchanged. Similar behaviour has been observed as phase transitions are approached in some other ferroelectrics, such as $BaTiO_3$ (Darlington *et al.*, 1994). This is somewhat contrary to the widely held notion that the ferroelectric distortion controls the crystal structure at all levels, *i.e.* that the lattice distortion should always scale with the ion positions and electric polarization. PZN has an extremely small distortion from cubic and yet has a large polarization, in contrast with, say, $PbTiO_3$, which has a large spontaneous strain but considerably smaller polarization. These observations indicate that, in ferroelectric materials, the relationship between the lattice parameters and atomic coordinates (and hence electric polarization) is more complex than in the non-ferroelectric perovskites.

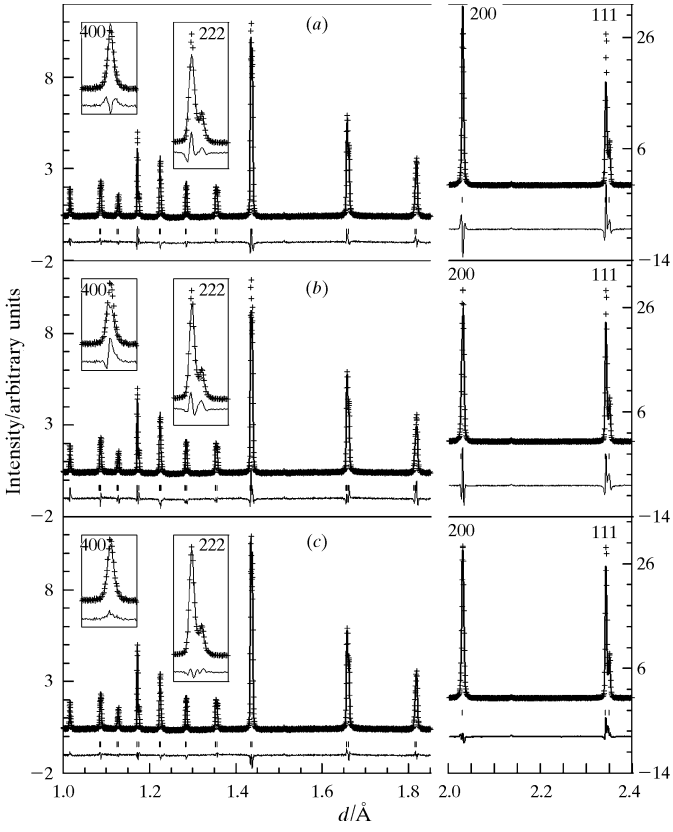

Figure 1
Results of Rietveld refinements using the 4.2 K data in the range 1–2.4 Å for models in (*a*) space group *R*3*m* without anisotropic broadening correction, (*b*) space group *Cm* and (*c*) space group *R*3*m* with the anisotropic broadening parameter S400 refined. Data are given as +, the calculated profile as a solid line and the difference profile as a solid line below. Vertical markers above the difference profile indicate the calculated Bragg reflection positions. Data in the range 2–2.4 Å are plotted according to the right-hand scale. Insets show details of the fit to the important 400 and 222 reflections.

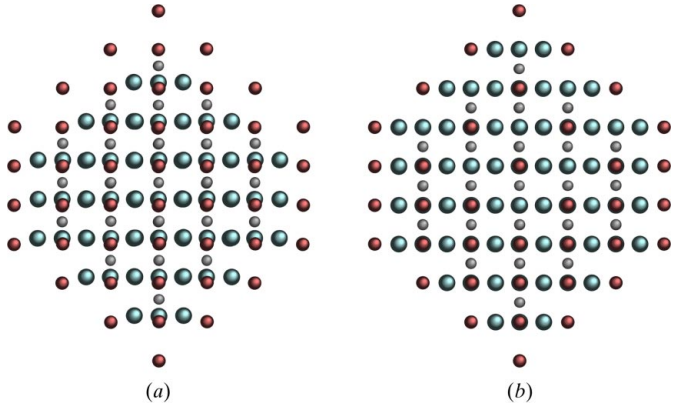

Figure 2
Views of (*a*) the 4.2 K structure and (*b*) the undistorted cubic structure, both projected perpendicular to the polar axis, [111].

Experimental

The flux growth method of Mulvihill *et al.* (1996) was used to grow single crystals of composition $Pb(Zn_{1/3}Nb_{2/3})O_3$. Crystals in the size range 0.5–15 mm were extracted from the flux in a hot HNO_3 solution. The chemical composition of the crystals and their homogeneity were verified using scanning electron microscopy-based energy dispersive spectroscopy (EDS) analysis. Using an agate pestle and mortar, crystals were lightly crushed to a size that passed through a coarse sieve (143 µm), so as to avoid strain and particle-size broadening. Good powder averaging was obtained using approximately 2 ml of powder sample.

Neutron powder diffraction patterns were recorded in transmission on the HRPD diffractometer (resolution $\Delta d/d \simeq 4 \times 10^{-4}$) at the ISIS facility, Rutherford Appleton Laboratory, England. Samples were held in a thin-walled aluminium can within a liquid helium cryostat. Diffraction patterns were recorded from 30 to 130 ms at room temperature and at 4.2 K for 20 and 90 min, respectively.

PZN at 4.2 K

Crystal data

$PbZn_{1/3}Nb_{2/3}O_3$
M_r = 337.40
Trigonal, *R*3*m*
a = 4.06048 (6) Å
α = 89.8693 (4)°
V = 66.95 (1) Å^3
Z = 1
D_x = 8.367 Mg m^{-3}
Time-of-flight neutron radiation
λ = 0.65–2.45 Å
T = 4.2 K
Specimen shape: powder
Specimen prepared at 101.3 kPa
Specimen prepared by cooling from 1473 to 1173 K at 1 K min^{-1} and at 50 K min^{-1} thereafter
Particle morphology: <143 μm particles, pale yellow

Data collection

HRPD beamline, ISIS, Didcot
Specimen mounting: 11 mm aluminium slab can
Scan method: time-of-flight

Refinement

R_p = 0.062
R_{wp} = 0.074
R_{exp} = 0.040
S = 2.48
Wavelength of incident radiation: 0.65–2.45 Å
Excluded region(s): none
Profile function: pseudo-Voight convoluted with double exponential incorporating the anisotropic microstrain broadening model of Stephens (1999)
34 parameters
$(\Delta/\sigma)_{max}$ = 0.01
Preferred orientation correction: none

PZN at 295 K

Crystal data

$PbZn_{1/3}Nb_{2/3}O_3$
M_r = 338.93
Trigonal, *R*3*m*
a = 4.06240 (8) Å
α = 89.8693 (4)°
V = 67.04 (1) Å^3
Z = 1
D_x = 8.396 Mg m^{-3}
Time-of-flight neutron radiation
λ = 0.65–2.45 Å
T = 295 K
Specimen shape: powder
Specimen prepared at 101.3 kPa
Specimen prepared at 101.3 kPa
Specimen prepared by cooling from 1473 to 1173 K at 1 K min^{-1} and at 50 K min^{-1} thereafter
Particle morphology: <143 μm particles, pale yellow

Data collection

HRPD beamline, ISIS, Didcot
Specimen mounting: 11 mm aluminium slab can
Specimen mounted in transmission mode
Scan method: time-of-flight

Refinement

R_p = 0.075
R_{wp} = 0.088
R_{exp} = 0.080
S = 1.49
Wavelength of incident radiation: 0.65–2.45 Å
Excluded region(s): none
Profile function: pseudo-Voight convoluted with double exponential incorporating the anisotropic microstrain broadening model of Stephens (1999)
37 parameters
$(\Delta/\sigma)_{max}$ = 0.03
Preferred orientation correction: none

Rietveld analyses used the program *GSAS* (Larson & Von Dreele, 1986). Data from the small crystal sample recorded by both the high-resolution backscattering bank and the high-intensity 90° detector bank were used simultaneously. Typically, lattice parameters, atom coordinates (Zn/Nb, O), isotropic displacement parameters (Zn/Nb), anisotropic displacement parameters (Pb, O), scale, eight polynomial background parameters and two peak profile parameters were used. The 4.2 K data were used to refine the Zn/Nb ratio of the *B* cation site and this ratio was held constant during refinements based on the 295 K data. In addition, the anisotropic peak-broadening model of Stephens (1999) was applied.

For both compounds, data collection: ISIS software (local programs); program(s) used to refine structure: *GSAS* (Larson & Von Dreele, 1986); molecular graphics: *CaRine Crystallography* (Bondias & Monceau, 2005) and *GRAPHER* (Golden Software, 2005); software used to prepare material for publication: *GSAS*.

The authors extend thanks to Dr Christopher Howard for reviewing the work prior to submission. This work was supported by the Australian Research Council and the Access to Major Research Facilities Programme.

Supplementary data for this paper are available from the IUCr electronic archives (Reference: FA1185). Services for accessing these data are described at the back of the journal.

References

Bondias, C. & Monceau, D. (2005). *CaRine Crystallography*. Distributed by Divergent SA, Compiegne, France.
Cox, D. E., Noheda, B., Shirane, G., Uesu, Y., Fujishiro, K. & Yamada, Y. (2001). *Appl. Phys. Lett.* **79**, 400–402.
Darlington, C. N. W., David, W. I. F. & Knight, K. S. (1994). *Phase Transitions*, **48**, 217–236.
Durbin, M. K., Jacobs, E. W., Hicks, J. C. & Park, S.-E. (1999). *Appl. Phys. Lett.* **74**, 2848–2850.
Frantti, J., Eriksson, S., Hull, S., Lantto, V., Rundlof, H. & Kakihana, M. (2003). *J. Phys. Condens. Matter*, **15**, 6031–6041.
Fu, H. & Cohen, R. E. (2000). *Nature (London)*, **403**, 281–283.
Golden Software (2005). *GRAPHER*. Golden Software Inc., Golden, Colorado, USA.
Kisi, E. H., Forrester, J. S. & Knight, K. S. (2005). *J. Phys. Condens. Matter*, **17**, L381–L384.
Kisi, E. H., Piltz, R. O., Forrester, J. S. & Howard, C. J. (2003). *J. Phys. Condens. Matter*, **15**, 3631–3640.
La-Orauttapong, D., Noheda, B., Ye, Z.-G., Gehring, P. M., Toulouse, J., Cox, D. E. & Shirane, G. (2002). *Phys. Rev. B*, **65**, 144101.
Larson, A. C. & Von Dreele, R. B. (1986). *GSAS*. Report LAUR 86-748. Los Alamos National Laboratory, New Mexico, USA.
Mulvihill, M. L., Park, S.-E., Risch, G., Li, Z., Uchino, K. & Shrout, T. R. (1996). *Jpn J. Appl. Phys.* **35**, 3984–3990.
Noheda, B., Cox, D. E. & Shirane, G. (2002). *Proceedings of the 10th International Meeting on Ferroelectrics* (IMF-10), Madrid, September 2001; published in *Ferroelectrics* (2002), **267**, 147–155.
Noheda, B., Cox, D. E., Shirane, G., Park, S.-E., Cross, L. E. & Zhong, Z. (2001). *Phys. Rev. Lett.* **86**, 3891–3894.
Noheda, B., Zhong, Z., Cox, D. E., Shirane, G., Park, S.-E. & Rehring, P. (2002). *Phys. Rev. B*, **65**, 224101.
Ohwada, K., Hirota, K., Rehrig, P. W., Gehring, P. M., Noheda, B., Fujii, Y., Park, S.-E. & Shirane, G. (2001). *J. Phys. Soc. Jpn*, **70**, 2778–2783.
Paik, D.-S., Park, S.-E., Wada, S., Liu, S.-F. & Shrout, T. R. (1999). *J. Appl. Phys.* **85**, 1080–1083.
Park, S.-E. & Shrout, T. R. (1997). *J. Appl. Phys.* **82**, 1804–1811.
Stephens, P. W. (1999). *J. Appl. Cryst.* **32**, 281–289.